

STRENGTH OF CRYOROLLED COMMERCIAL HEAT HARDENABLE ALUMINUM ALLOY WITH MULTILEVEL NANOSTRUCTURE

S. V. Krymskiy, O. Sh. Sitdikov, E. V. Avtokratova, M. Yu. Murashkin
and M. V. Markushev

Institute for Metals Superplasticity Problems RAS, 39 Khalturin St., Ufa, Russia
Institute of Physics of Advanced Materials, USATU, 12 K. Marx St., Ufa, Russia

Received: April 20, 2012

Abstract. It has been found that cryorolling of the preliminary quenched commercial rod of D16 aluminum alloy at a temperature of liquid nitrogen up to strains of 3.5 results in the well-developed cellular substructure with separate nanograins inside coarse fibers. Further aging at ambient and elevated temperature leads to the alloy disperse strengthening accompanied by recovery and recrystallization of the deformation structure. After natural aging the cryorolled alloy demonstrates much higher strength ($YS = 635$ MPa) and hardness (~ 180 Hv) but less plasticity ($EI < 3\%$) than in conventionally T6 treated material. Meanwhile, the artificially aged alloy exhibits the unique balance of strength ($YS = 570$ MPa) and plasticity ($EI > 7\%$) reasoned by its multilevel nanostructuring, owing to the formation of mixed nanoprecipitation- and nano(sub)grain-strengthened structure.

1. INTRODUCTION

Development of new methods for strengthening of metallic materials has caused appreciable interest in their straining at cryogenic temperatures [1]. Such processing of pure metals and solid solutions usually results in well-developed deformation structures accompanied by their enhanced strength at room temperature [1,2]. The latter is caused by the «structural» hardening owing to two predominant factors – grain refinement (fragmentation) and the formation of high-density dislocation structures. Recent investigations have also been found a great potential of low-temperature severe plastic deformation (SPD) (with the strains exceeding $\epsilon \sim 2-3$) for processing the nanocrystalline structures with unique strength in as-deformed condition [2-8] as well as with unique balance of strength and plasticity after

further annealing [3,4,8-12]. In this connection, it is of great interest to evaluate the efficiency of SPD processing at cryogenic temperatures for precipitation-hardened material, to establish its strengthening limit resulting from changes in both the structure of the matrix and the phase constituents; *i.e.*, to study the synergetic effect on structural and dispersional hardening during straining and subsequent annealing in the temperature range of natural-artificial aging of the material such as heat-hardenable aluminum alloy.

2. MATERIAL AND PROCEDURE

The structure-property relationships were analyzed for commercial middle-strength aluminum alloy D16 (Al-4.4%Cu-1.4%Mg-0.7%Mn). The material under the study was in the form of plates of 5 mm thick,

Corresponding author: S. V. Krymskiy, e-mail: stkr_irmsp@mail.ru

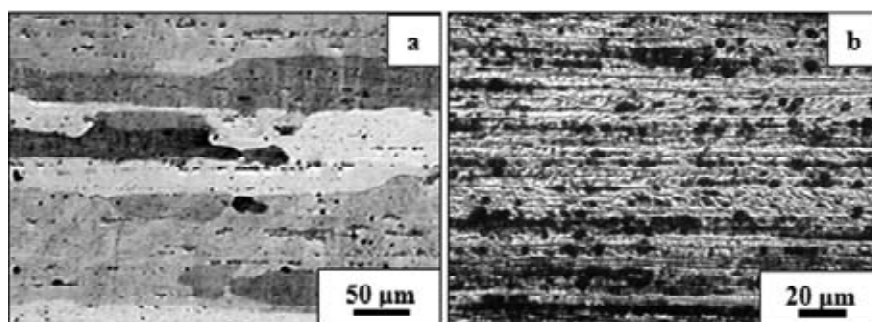


Fig. 1. Microstructures of the D16 alloy in the longitudinal cross-section of the hot-pressed rod (a) and cryorolled with a strain ~ 3.5 sheet (b).

which were cut along the axis of the conventionally hot-pressed rod, solution-treated at 500 °C, water-quenched and then rolled up to strains $e \sim 3.5$ in isothermal conditions at a temperature of liquid nitrogen (CR condition). After rolling the plates were naturally aged for 6 days (CR+NA condition) or artificially aged up to 48 hrs at temperatures up to 190 °C (CR+AA condition). For property comparison, the initial and cryorolled material was also subjected to T6 conventional strengthening heat treatment: water quenching from 500 °C and aging at 190 °C, 12 hrs [13] and these alloy conditions were designated as T6 and CR+T6, respectively. Besides, the cryorolled and aged at 190 °C for 12 hrs alloy (i.e. in accordance with T6 regime) was designated as CR+AA(T6).

The dislocation and grain structures of the matrix (aluminum solid solution) as well as phase composition of the alloy before and after cryorolling were studied by standard methods of optical and transmission electron microscopy (OM and TEM), and X-ray diffraction (XRD) analysis. Metallographic observations were carried out using a Nikon L-150 optical microscope and templates with pre-polished and etched in the Keller's reagent surface. TEM examinations were performed in the JEOL-2000EX electron microscope. Objects for analysis were mechanically ground to a thickness of about 200 μm and electro-polished at 20 V in a solution of 30 pct HNO_3 and 70 pct CH_3OH at a temperature of -30 °C using a Tenupol-6 device. The coherent domain size, microstrain and lattice parameter of the matrix were determined with the help of the DRON-4 XRD analyzer.

The alloy room temperature tensile strength parameters (yield and ultimate tensile strength (YS and UTS) and elongation to failure (EI)) were measured in compliance with the Russian State standard using Instron 1185 testing machine and samples with a gage part of 5x15x0.6 mm. The

microhardness (Hv) was evaluated by MHT-10 Vickers hardness tester with a load of 100 g on the diamond pyramid indenter.

To obtain the average value of each parameter with sufficient accuracy five to ten measurements have been made.

3. RESULTS AND DISCUSSION

OM and TEM (Figs. 1 and 2) have shown that cryorolling does not qualitatively change the type of structure of the alloy matrix. Even after severe straining to $e \sim 3.5$ it remains coarse-fibered, as in the initial quenched rod (Fig. 1). Cryorolling has led only to further elongation of fibers and decrease in their thickness accompanied by microshear banding and substitution of the hot-pressed polygonized substructure (Fig. 2a) by the well-developed cellular one with high densities of randomly distributed lattice dislocations (Figs. 2b-2d). It should be noted that transition from conventional ($e \sim 0.9$) to severe ($e \sim 3.5$) straining did not result in a considerable decrease in the cell size, remaining in a range of ~ 100 -200 nm. However, TEM images of cell boundaries became sharper and less blurred with strain (Fig. 2), suggesting increase in their misorientations. Meanwhile, only insignificant fraction of boundaries has demonstrated a contrast typical for non-equilibrium boundaries in nanocrystalline materials produced by ambient temperature SPD [4,14]. So, it should be noted that the CR alloy structure after straining to 3.5 is qualitatively similar to the structures formed by conventional cold-rolling or SPD-processing with rather small ($e < 2$) effective strains realized, for example, by accumulative roll-bonding [14,15] or equal-channel angular pressing [16,17]. Thus, cryorolling at mentioned above conditions resulted in the initial stage of the alloy nanocrystalline structure formation only. In that stage initiation of separate strain-induced nano(sub)grains with size less

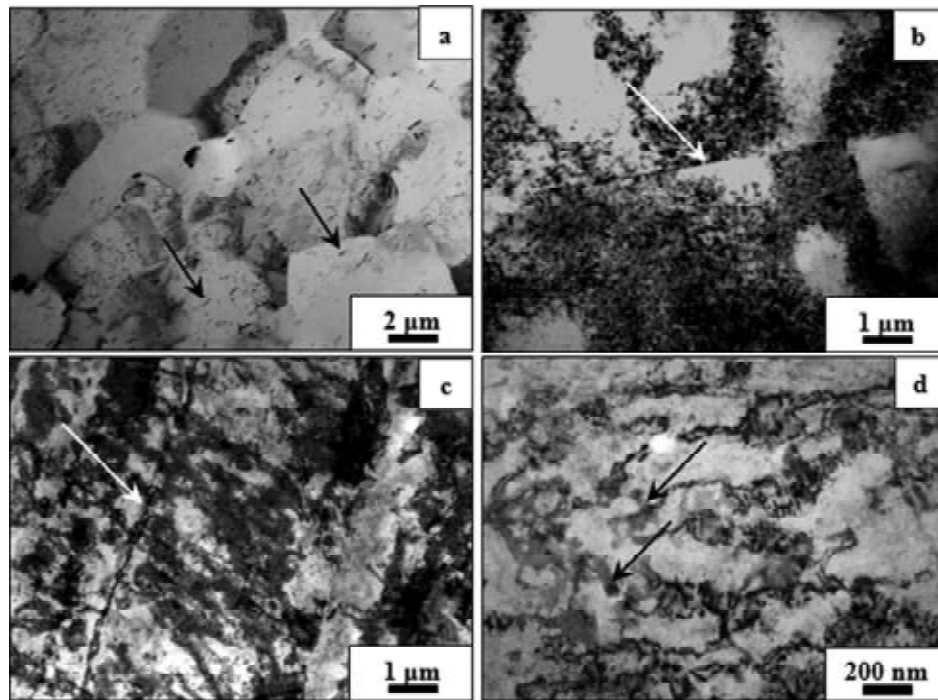


Fig. 2. TEM structures of the D16 alloy in the hot-pressed (a) and further cryorolled with a strain ~ 0.9 (b), 2.0 (c) and 3.5 (d) conditions. White arrows indicate “old” boundaries of the initial fibers, black arrows – particles of T-phase ($\text{Al}_{20}\text{Cu}_2\text{Mn}_3$). (a- longitudinal plane of the rod, b-d – rolling plane of the sheet).

than 100 nm and volume fraction not exceeding 10% is observed. Therefore, such a structure can be considered as nanostructure if taking the cell size for a determining structural parameter.

It should be also noted that the alloy matrix in the initial quenched state was strengthened by homogeneously distributed secondary dispersed particles of T-phase ($\text{Al}_{20}\text{Cu}_2\text{Mn}_3$), stabilizing its dislocation structure under processing (Fig. 2a). It is clearly seen that such dispersoids remain TEM visible in the alloy cryorolled to all the strains investigated (see, for instance, Fig. 2d), testifying the absence of their considerable dissolution under straining. Moreover, it is also necessary to note that the analysis of the data presented in [18-20] and in the present paper, has testified to the absence of any significant TEM and XRD detectable observations of decomposition of the aluminum solid solution or dissolution of any primary or secondary phases during cryorolling.

XRD analysis has also shown that the coherent domain size (coherent-scattering area) evolves with rolling strain, resulting in its significant reduction from 130-135 to 50-60 nm and further stabilization at that level after straining to $e > 0.9$ (Fig. 3a). The behavior is practically similar to that of matrix cell size in response to strain. On the contrary,

microstrain of the matrix first increases more than thrice from ~ 0.07 to $\sim 0.24\%$ at $e \sim 0.5$, and then slightly rises to $\sim 0.34\%$ (Fig. 3b), which testifies for sharp increase in the alloy dislocation density in the initial stage of deformation followed by the formation and slight transformation of its cellular structure. At the same time more complex behavior was found for lattice parameter of the matrix, starting with strong decrease from 4.053 to 4.048 Å at straining to $e \sim 0.2$, and followed by its monotonic reversion with strain to the typical for T6 conventionally heat hardened material value of 4.052 Å (Fig. 3c).

All the revealed structural changes have influenced the parameters of the alloy mechanical behavior, involving hardness, the evolution of which under cryorolling has been shown in Fig. 3d. In particular, the major changes in the alloy structure have been found at straining to ~ 1 , correspondingly the significant increase in the alloy hardness was observed. It was conditioned by strong changes in dislocation structure of the alloy matrix leading to the formation of developed cell structure. Because of absence of any «important» structural transformations in the aluminum solid solution at processing to higher strains, no sense increase in the alloy hardness has been found. Obviously, next qualitative change in its behavior should be reasoned by

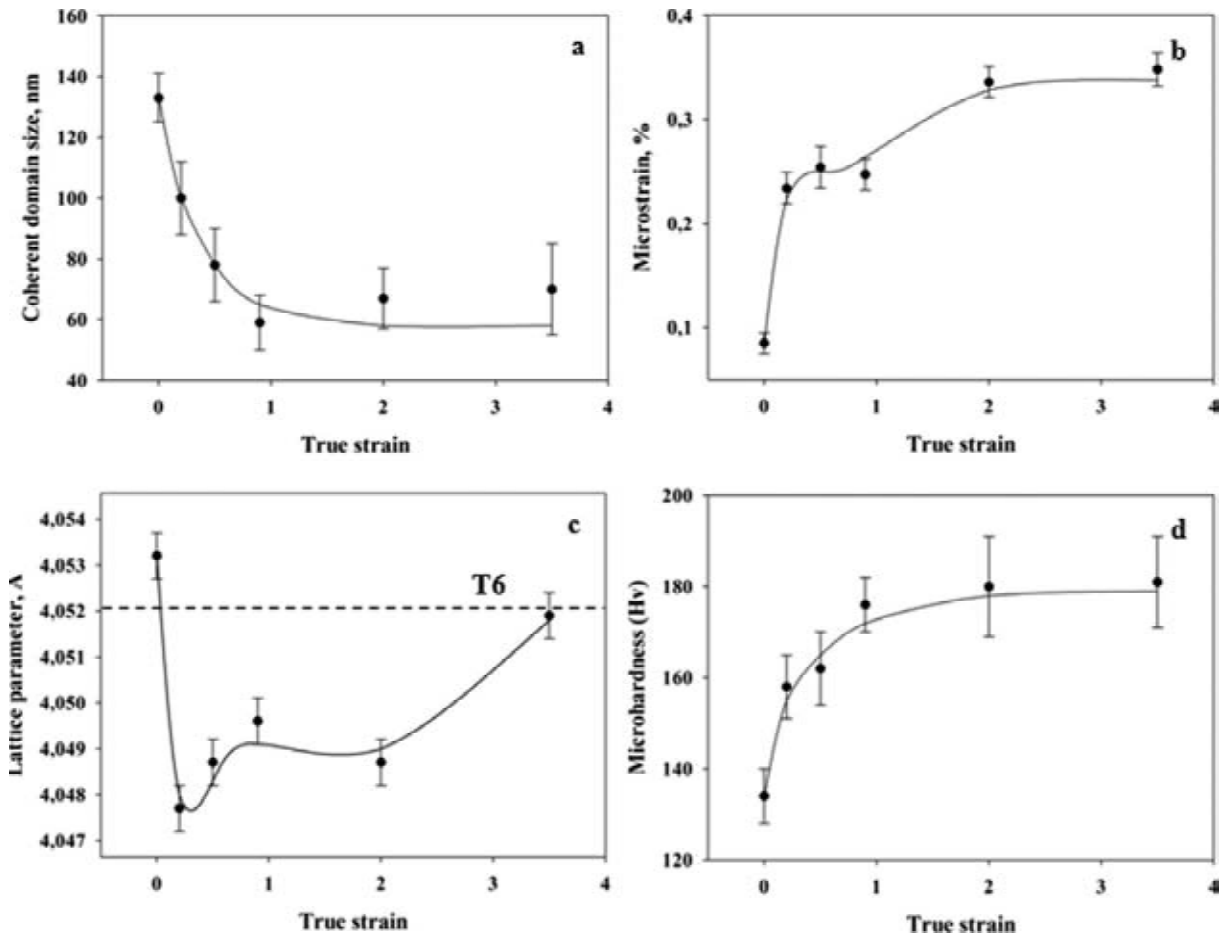


Fig. 3. Dependencies of the coherent domain size (a), microstrain (b), lattice parameter (c) and microhardness (d) of the D16 alloy on strain of the cryorolling.

the formation of NC structure. However, owing to the data presented, it is hard to be realized due to requirements of much higher strains than under this study.

The peculiarities of the alloy deformation structure and hardness evolution with strain suggest finding another way of property-structure control based on precipitation strengthening of the matrix, i.e. on the alloy phase transformations. It was another extremely important reason to examine the mentioned above effect of cryorolling on the alloy phase composition and lattice parameter of the preliminary oversaturated aluminum solid solution, and to find out any features of the alloy dynamic aging.

Basing on the TEM and XRD data it has been concluded that the decomposition of aluminum solid solution, accompanied with initiation and growth of zones and S- and θ -phase (Al_2CuMg and Al_2Cu) precipitates inside the highly work-hardened matrix, occurs during post-deformation natural and artificial aging. Simultaneously, softening processes of static recovery and recrystallization take place (preferably at artificial aging) leading to changes in the alloy

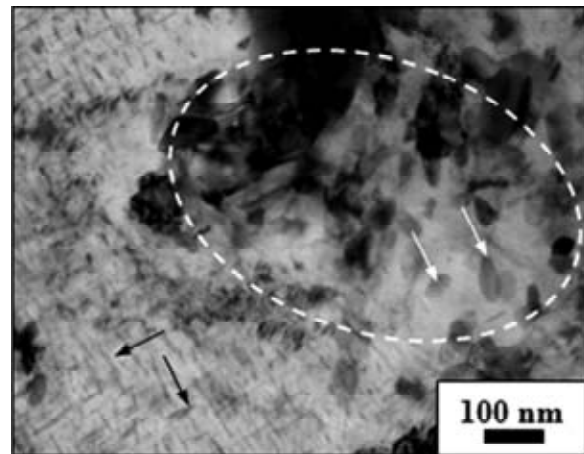


Fig. 4. TEM structure of the D16 alloy after cryorolling with $e \sim 2$ and artificial aging at 190 °C for 12 hrs. White circle indicate area with recrystallized nano(sub)grain structure, black arrows - needle(disc)-like S-phase precipitates, white arrows - compact precipitates.

matrix structure. Commonly, the structure transforms into more equilibrium one with nanoprecipitates inside cells, subgrains and grains,

Table 1. Tensile strength parameters of the D16 alloy at a room temperature.

Condition	YS, MPa	UTS, MPa	EI, %
T6	390	440	7.0
CR + NA	635	645	3.0
CR + AA (T6)	450	495	5.9
CR + AA (developed)	570	635	8.8
CR + T6	380	475	14.1

T6 – quenching from 500 °C and aging at 190 °C, 12 hrs, CR – cryorolling with $e \sim 2$, NA – natural aging for 6 days, AA – artificial aging

gradually getting features of nanostructure of grain type with increase in temperature and time of aging. However, under the regimes of artificial aging investigated, the crystal structure of the matrix predominantly remains bimodal consisting of both recovered and recrystallized areas. Such a bimodal structure, for instance, is shown in Fig. 4 for cryorolled and aged at 190 °C for 12 hrs (CR + AA(T6)) alloy. Its first mode is presented by cell/dislocation structure with needle (disc)-like precipitates ~ 2 -10 nm thick and up to ~ 100 nm long (in Fig. 4 indicated by black arrows). The second mode - by nano/ultrafine (sub)grains with compact slightly elongated precipitates 10-50 nm in size (in Fig. 4 indicated by white circle and white arrows, consequently). Thus, aging of cryorolled material leads to the formation of multilevel nanostructure characterized by at least of two nanosized phase constituents, their specific volume fractions, morphology and spectrum of grain and interphase boundaries.

Owing to the absence of significant structural transformations in the alloy at strains higher than two and consequent microhardness saturation, tensile tests were performed for cryorolled condition with $e \sim 2$ only. It has been revealed that rolling and further natural aging for a period of samples preparation (~ 6 days) led to the alloy ultrahigh strength (YS = 635 MPa and UTS = 645 MPa), exceeding the level in both heat hardened to T6 tempers conventionally processed and cryorolled sheets, but low plasticity (EI ≤ 3 %) (Table 1). Such property balance is conditioned by strong work hardening and the formation of highly defect structure of the matrix, described above. Subsequent artificial aging of the rolled material under T6 regimes (190 °C, 12 hrs) led to somewhat enhancement in its plasticity. However, it was accompanied by the alloy strength decrease to conventional values (Table 1). Such a behavior is reasoned by the recovery and recrystallization of the matrix and the formation of the overaged precipitation structures [13] in recovered

areas and quite coarse compact particles of stable strengthening phases of low densities in recrystallized ones (Fig. 4). The latter is due to two factors, first - more intense growth (coagulation) rate of strengthening phases in a highly work-hardened (highly defect) matrix, second – changes in the morphology of precipitates (predominantly in the structure of interphase boundaries and particles shape) caused by simultaneous initiation of precipitates, their growth and changes in their crystallographic orientations owing to recrystallization processes of the surrounding matrix.

However, it was found that aging under non-standard regimes could provide much better balance of the alloy strength and plasticity (Table 1). The effect is conditioned by less softening of the deformation structure during annealing due to less intense recovery and recrystallization of the aluminum solid solution. Obviously, it is also reasoned by the development of more disperse and uniformly distributed strengthening phases inside the both matrix structural modes, practically without formation of precipitate free zones along high- and low-angle boundaries.

Thus, the D16 alloy sheets with unique strength and/or balance of room temperature mechanical properties can be processed by combination of cryorolling and strengthening heat treatment, leading to formation of multilevel nanostructure characterized by specific mixture of nano(sub)grains and nanoprecipitates, that is, with specific combination of nano-sized phase constituents – crystallites of aluminum solid solution and particles of secondary aluminides.

4. CONCLUSIONS

1. Room temperature tests have revealed that the D16 alloy in isothermally cryorolled at a liquid nitrogen temperature with a strain of $e \sim 2.0$ and naturally aged condition demonstrates the unique

strength parameters (YS = 635 MPa and UTS = 645 MPa) and hardness (~180 Hv) much higher than in the T6 processed sheet, accompanied, however, by low plasticity ($EI \leq 3\%$). Further artificial aging of the alloy under conventional regimes (as in T6) led to its rather enhanced plasticity with strength and hardness decrease to conventional values.

2. Post-rolling artificial aging activates recovery and continuous recrystallization, and results in simultaneous two-level nanostructuring of the alloy with the formation of mixed nanoprecipitation- and nano(sub)grain-strengthened structure. Formation of the alloy structure of such type upon aging under the regimes developed led to the unique balance of its strength and plasticity (YS = 570 MPa, UTS = 635 MPa, $EI > 7\%$).

The work was supported by the Ministry of Education and Science of the Russian Federation (Grant N 14.740.11.0278).

REFERENCES

- [1] P.A. Khaimovich // *Prob. Atomic Sci. Technology* **4** (2006) 28.
- [2] V.A. Moskalenko and A.R. Smirnov // *Phys. Low. Temp.* **35** (2009) 1160.
- [3] E. Ma // *JOM* **58** (2006) 49.
- [4] R.A. Andrievskiy and A.M. Glezer // *Phys. Usp.* **52** (2009) 315.
- [5] J. Yin, J.Lu, H. Ma and P. Zhang // *J. Mater. Sci.* **39** (2004) 2851.
- [6] Y.S. Li, N.R. Tao and K. Lu // *Acta Mater.* **56** (2008) 230.
- [7] T. Konkova, S. Mironov, A. Korznikov and S.L. Semiatin // *Acta Mater.* **58** (2010) 5262.
- [8] S.K. Panigrahi and R. Jayaganthan // *Mat. Sci. Forum.* **584–586** (2008) 734.
- [9] S. Cheng, Y.H. Zhao, Y.T. Zhu and E. Ma // *Acta Mater.* **55** (2007) 5822.
- [10] Y.B. Lee, D.H. Shin, K.T. Park and W.J. Nam // *Scripta Mater.* **51** (2004) 355.
- [11] Y.H. Zhao, X.Zh. Liao, Sh. Cheng and E. Ma // *Adv. Materials.* **18** (2006) 2280.
- [12] T. Shanmugasundaram, B.S. Murty and V. Subramanya Sarma // *Scr. Mater.* **54** (2006) 2013.
- [13] Z.N. Archakova, G.A. Balakhontsev and I.G. Basova, *Structure and Properties of Semiproducts Made of Aluminum Alloys* (Metallurgiya, Moscow, 1984), in Russian.
- [14] R.Z. Valiev and I.V. Aleksandrov, *Bulk Nanostructured Materials: Production, Structure, and Properties* (Akademkniga, Moscow, 2007), in Russian.
- [15] H.R. Song, Y.S. Kim and W.J. Nam // *Met. Mater. Int.* **12** (2006) 7.
- [16] V.M. Segal, V.I. Reznikov and V.I. Kopylov, *Processes of Plastic Structure Formation in Metals* (Navuka i Tekhnika, Minsk, 1994), in Russian.
- [17] M. Murayama, Z. Horita and K. Hono // *Acta mater.* **49** (2001) 21.
- [18] M.V. Markushev, E.V. Avtokratova and I.Ya. Kazakulov // *Russian Metallurgy (Metally)* **4** (2011) 364.
- [19] S.V. Krymskiy, E.V. Avtokratova and M.V. Markushev // *Mater. Sci. Forum* **667-669** (2011) 925.
- [20] E.V. Avtokratova, S.V. Krymskiy, M.V. Markushev and O.Sh. Sitdikov // *Letters on Mat.* **1** (2011) 92, in Russian.